

vary as  $r \propto (t_0 - t)^{1/2}$  where  $t_0$  is the time at which the loop disappears. The disclination wall will carry some excess energy per unit length which, by integration over the  $\varphi(X)$  resulting from Eq. (2), is given by  $U_w = 8K/\xi \propto E^{1/2}$ .  $U_w$  has dimensions of force and may be viewed as an effective line tension acting on the wall locally tangent to it. The effective normal force per unit length,  $f$ , will be  $f = U_w/r$  where  $r$  is the local radius of curvature. The disclination wall will move under this force which in steady state will be balanced by a viscous force per unit length,  $f_v = -\beta\dot{r}$ , arising because motion of the wall past a point on the film is accompanied by dissipative molecular rotation. Equating the two forces gives the equation  $\dot{r}(t) = -(U_w/\beta)/r(t)$  for the local motion of a wall. This yields  $r^2(t) = (2U_w/\beta)(t_0 - t)$  for a circular loop which is what we observe. Detailed calculation shows that  $\beta = 8\eta/\xi$  where  $\eta$  is a 2D orientational viscosity. Hence the collapse rate constant  $U_w/\beta = K/\eta$  independent of  $E$ . Our experimental results for  $K/\eta$ , obtained from the slope of the  $r^2$  vs  $(t_0 - t)$  curves, are  $K/\eta = 9.2$  ( $N=2$ ),  $7.3$  ( $N=3$ ),  $6.2$  ( $N=4$ ), and  $5.0$  ( $N=5$ ); all are  $\pm 1.0$  in units of  $10^{-5}$  cm<sup>2</sup>/sec. These lie between  $K_b/\eta_b$  and  $K_s/\eta_s$  previously obtained from light

scattering<sup>2</sup> and are independent of  $E$  as expected.

We would like to acknowledge the assistance of P. S. Pershan, C. S. Rosenblatt, and W. Chan. This work was supported in part by the National Science Foundation under Grants No. 76-22452, 79-20169, and the National Science Foundation-Materials Research Laboratory Program Grant No. DMR-76-01111.

<sup>1</sup>G. Friedel, *Ann. Phys. (Paris)* **18**, 273 (1922).

<sup>2</sup>C. Y. Young, R. Pindak, N. A. Clark, and R. B. Meyer, *Phys. Rev. Lett.* **40**, 773 (1978).

<sup>3</sup>J. M. Kosterlitz and D. J. Thouless, *J. Phys. C* **6**, 1181 (1973); R. A. Pelcovits and B. I. Halperin, *Phys. Rev. B* **19**, 4614 (1979); D. R. Nelson and B. I. Halperin, *Phys. Rev. B* (to be published).

<sup>4</sup>R. B. Meyer, L. Liebert, L. Strzelecki, and P. Keller, *J. Phys.* **36**, L69 (1975).

<sup>5</sup>Since between  $\varphi = \pm\pi/2$  the wall contains equal amounts of bend and splay distortion, it is the average elastic constant  $K = \frac{1}{2}(K_b + K_s)$  that determines  $w$ . Any difference between  $K_s$  and  $K_b$  is a negligibly small correction.

<sup>6</sup>C. Rosenblatt, R. Pindak, N. A. Clark, and R. B. Meyer, *Phys. Rev. Lett.* **1220** (1979). DOBAMBC refers to *p*-decyloxybenzylidene *p'*-amino 2-methylbutyl cinamate.

## Crystal Structure and Pair Potentials: A Molecular-Dynamics Study

M. Parrinello<sup>(a)</sup> and A. Rahman

*Argonne National Laboratory, Argonne, Illinois 60439*

(Received 31 July 1980)

With use of a Lagrangian which allows for the variation of the shape and size of the periodically repeating molecular-dynamics cell, it is shown that different pair potentials lead to different crystal structures.

PACS numbers: 61.20.Ja, 05.70.Fh, 61.50.Cj, 64.70.Dv

Recent molecular-dynamics (MD) calculations<sup>1</sup> on homogeneous nucleation of a crystal out of a supercooled liquid phase have shown that the structure of the nucleated phase does depend on the pair potential. These calculations are time consuming because of the long-lived, glassy, metastable states which the system has to inhabit before nucleating. Here we present a very direct and relatively short calculation which relates the crystal structure to the pair potential in a simple manner.

Andersen<sup>2</sup> has shown how MD calculations can be modified to study systems under constant pres-

sure by introducing the volume of the system as an additional dynamical variable. In this paper we show how a generalization of this idea leads to a powerful method for the study of crystal structures and their relation to pair potentials. We have performed MD calculations with a time-dependent metric tensor which allows the volume and the shape of the MD cell to vary with time.

Let the edges of the MD cell be  $\vec{a}$ ,  $\vec{b}$ , and  $\vec{c}$  (in a space-fixed coordinate system), and let them be time dependent. Periodically repeating MD cells will obviously fill up all space. Let  $\underline{h}$  be the matrix formed by  $\{\vec{a}, \vec{b}, \vec{c}\}$ ;  $\Omega = \det \underline{h} \equiv \vec{a} \cdot \vec{b} \times \vec{c}$

will then be the volume of the MD cell containing, say  $N$  particles. The position of particle  $i$  will be  $\vec{r}_i = \xi_i \vec{a} + \eta_i \vec{b} + \zeta_i \vec{c} = \underline{h} \vec{s}_i$ , where  $\vec{s}_i$  has components  $(\xi_i, \eta_i, \zeta_i)$  each going from 0 to 1. Obviously  $r_i^2 = \vec{s}_i' \underline{G} \vec{s}_i$ , where  $\underline{G} = \underline{h}' \underline{h}$ , the transpose being denoted by a prime. Using a dot to denote time derivatives, we write the Lagrangian

$$L = \frac{1}{2} \sum_i m_i \dot{\vec{s}}_i' \underline{G} \dot{\vec{s}}_i - \sum_i \sum_{j>i} \varphi(r_{ij}) + \frac{1}{2} W \text{Tr}(\dot{\underline{h}}' \dot{\underline{h}}) - p_{\text{ext}} \Omega. \quad (1)$$

Obviously  $r_{ij}^2 = (\vec{s}_i - \vec{s}_j)' \underline{G} (\vec{s}_i - \vec{s}_j)$ ;  $p_{\text{ext}}$  denotes the externally applied hydrostatic pressure;  $\varphi(r)$  is the pair potential; the kinetic term associated with the time variation of  $\underline{h}$  has a constant of proportionality  $W$  which has the dimension of mass.

With use of  $\chi(r)$  to denote  $-d\varphi/rdr$ , the Lagrangian equations of motion are easily written down:

$$\ddot{\vec{s}}_i = m_i^{-1} \sum_{j \neq i} \chi(r_{ij}) (\vec{s}_i - \vec{s}_j) - \underline{G}^{-1} \underline{\dot{G}} \dot{\vec{s}}_i, \quad (2)$$

$$i, j = 1, 2, \dots, N,$$

$$\ddot{\underline{h}} = W^{-1} (\underline{\pi} - p_{\text{ext}} \underline{\sigma}). \quad (3)$$

The matrix  $\underline{\sigma}$  has elements  $\sigma_{ij} = \delta\Omega/\delta h_{ij}$ ; the matrix  $\underline{\pi}$  is given in dyadic tensor notation by

$$\Omega \underline{\pi} = \sum_i m_i \vec{v}_i \vec{v}_i + \sum_i \sum_{j>i} \chi(r_{ij}) (\vec{r}_i - \vec{r}_j) (\vec{r}_i - \vec{r}_j), \quad (4)$$

the vector  $\vec{v}_i$  being  $\dot{\underline{h}} \vec{s}_i$ . Equations (2) and (3) govern the dynamics of a system of  $N$  particles in a periodically repeating MD cell which changes with time in shape and volume. Equation (3) is the expected relation between the variation of  $\underline{h}$ , the microscopic stress tensor  $\underline{\pi}$ , and the external pressure;  $\underline{\pi}$  and  $p_{\text{ext}}$  act across the various areas given by the components of  $\vec{b} \times \vec{c}$ ,  $\vec{c} \times \vec{a}$ , and  $\vec{a} \times \vec{b}$ , which make up  $\underline{\sigma}$ . In Eq. (3) we clearly see the possibility of a generalization to a nondiagonal external stress tensor.

In the special case of Andersen<sup>2</sup>  $\underline{h} = \text{diag}(\Omega^{1/3}, \dots, \Omega^{1/3})$  and  $\underline{G}^{-1} \underline{\dot{G}} = 2\dot{\Omega}/3\Omega$ , but his equation for  $\ddot{\underline{\Omega}}$  cannot be obtained from Eq. (3). However, as in Andersen,<sup>2</sup> it is easy to show that  $L$  of Eq. (1) generates an isoenthalpic, isobaric ensemble, apart from a small correction arising from the term in  $W$ .

We have used Eqs. (2) and (3) to investigate the Lennard-Jones 6-12 potential  $V_{\text{LJ}}$  and a pair potential<sup>3</sup> suitable for rubidium metal  $V_{\text{Rb}}$ .<sup>4</sup> Units of length, mass, and energy are chosen<sup>1</sup> in the

standard fashion, so that all quantities carrying an asterisk are the so-called reduced variables.

The MD calculation is started with a 500-particle system forming an fcc structure in a cubic cell of length  $l^* = 8.046$  appropriate to the number density  $\rho^* = 0.96$ . Thus at the start  $\underline{h} = \text{diag}(l^*, \dots, l^*)$ . A small random displacement of each particle from its lattice site provides the initial conditions for the ensuing dynamics; the MD time step was taken to be  $\Delta t^* = 0.005$ . The structure was monitored through the pair correlation function  $g(r)$ .

The summary of one of several calculations is given in Fig. 1 and described in the following. In this calculation we used  $W^* = 20$ .<sup>5</sup> At  $t = 0$   $V_{\text{Rb}}$  was taken as the pair potential and  $p_{\text{ext}}$  was taken as 4.0.<sup>6</sup> Using well-known MD techniques, the temperature of the system was set at a value  $T^* = 0.15$  for a duration of 140 MD steps. Since the starting structure was fcc the pair correlation during this time showed clear and sharply defined shells at distances relevant to an fcc structure, namely 1,  $\sqrt{2}$ ,  $\sqrt{3}$ ,  $\sqrt{4}$ , etc. [see Fig. 1,  $g(r)$  at  $t^* = 0$ ]. However, at step 400 ( $t^* = 2$ ) it already became evident that the MD cell was undergoing a secular modification toward a rectangular parallelepiped with two edges  $\vec{a}, \vec{b}$  of about the same length and a shorter third edge  $\vec{c}$  [see Fig. 1, where  $(a+b)/2c$  is seen to be starting to increase with time almost as soon as the calculation starts]. The nondiagonal elements of  $\underline{h}$  showed small fluctuations around zero. The volume, apart from small fluctuations, showed no secular change. After 2000 MD steps ( $t^* = 10$ ) the structure of the system had changed from fcc to bcc [in Fig. 1 see  $g(r)$  at  $t^* = 14$ ]. The bcc structure so obtained showed no sign of any secular change for another 1500 time steps. (It is to be noted that a body-centered tetragonal lattice with edges 1, 1, and  $\sqrt{2}$  is an fcc structure and, inversely, a tetragonal face-centered structure with edges  $\sqrt{2}$ ,  $\sqrt{2}$ , and 1 is a bcc structure. An hcp structure also can be generated out of a body-centered tetragonal structure by appropriate changes of lengths, angles and the position of the body center.)

At this time,  $t^* = 17.5$ , the pair potential was changed from  $V_{\text{Rb}}$  to  $V_{\text{LJ}}$  and simultaneously  $p_{\text{ext}}$  was put to zero (which is the value appropriate for this potential at  $\rho^* \sim 1.0$ ). At the moment of the change of potential the stable body-centered structure occupied an MD cell with sides 9.00, 9.02, and 6.41, and angles within  $1^\circ$  of being right angles. Immediately after the change, the cell

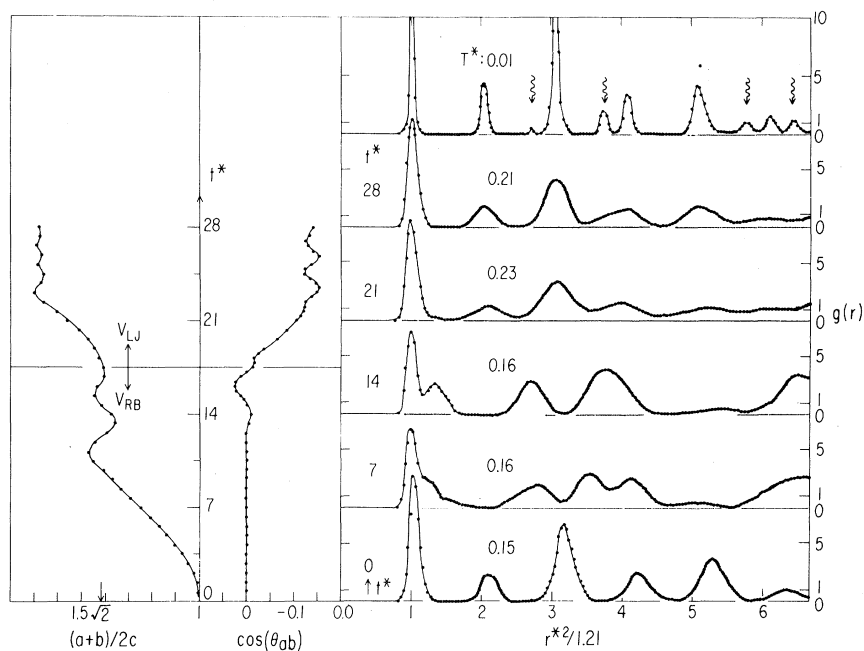


FIG. 1. The first graph on the left-hand side shows the MD cell edges  $\{\vec{a}, \vec{b}, \vec{c}\}$  as a function of time  $t^*$ . The ratio  $(a+b)/2c$  has been plotted; it is unity at  $t^*=0$ . When the potential is  $V_{RB}$  and the MD cell is cubic; it tends to  $\sqrt{2}$  with the passage of time. When  $V_{RB}$  is changed to  $V_{LJ}$  at  $t^*=17.5$ , further changes occur in  $\{\vec{a}, \vec{b}, \vec{c}\}$  accompanied by a change of the angle between  $\vec{a}$  and  $\vec{b}$ . The cosine of this angle is shown as a function of time in the second graph from the left. The various times at which the  $g(r)$  was monitored are indicated on the series of graphs on the right; each  $g(r)$  is an average over 140 time steps; the average temperature during these time steps is also shown. The final state when quenched reveals, in the topmost figure, subsidiary peaks (wiggly arrows) due to stacking faults mentioned in the text. Note that  $g$  is plotted as a function of  $r^2$ . The ratio of the squares of shell distances is 1:2:3:4:5:6, etc., in an fcc lattice and 1:4/3:8/3:11/3:4:16/3:19/3:20/3, etc., in a bcc lattice.

and the structure started to deform. In about 1000 more time steps (i.e., at  $t^*=25$ ) a new shape of the MD cell and a new  $g(r)$  were established. The cell parameters became 9.54, 9.23, and 5.59 with an angle of  $98^\circ$  between the first two, the third being essentially perpendicular to them. The system acquired a density  $\rho^*=1.03$ . In Fig. 1 is shown the  $g(r)$  at  $t^*=28$ . The first two peaks in  $g(r)$  correspond to a close-packed structure. When the final configuration was quenched to  $T^*=0.01$  with a short 100 step run, it revealed low-intensity peaks in  $g(r)$  which would be absent in a perfect fcc stacking [see last  $g(r)$  in Fig. 1]. A visual examination of the stacking along the direction of close packing revealed the order *ABABCACBA* and hence the stacking faults. In Fig. 1 the history of the run is depicted in a way as to reveal the changes in the MD cell parameters and in  $g(r)$  with the passage of time.

In recent years increasing attention has been given to the problem of predicting the crystalline

phase of a system<sup>7</sup> with known particle interactions. For most ionic materials, a fairly coherent idea already exists concerning the lattice structure on the one hand and ionic sizes and charges on the other.<sup>8</sup> However, for monatomic systems and short-range, pairwise, central forces, which lattice is favored by the system at a certain density and temperature is in practice not an easy question to answer, except at temperatures low enough to allow a harmonic approximation to be valid.

We have shown here that the Lagrangian of Eq. (1) is a powerful tool for studying phase transitions in solids, especially in relation to the form of particle interactions. Monte Carlo studies of  $(N, p, T)$  ensembles generated by the two potential terms in Eq. (1) with  $N+3$  vectors  $\vec{a}, \vec{b}, \vec{c}$ , and  $\vec{s}_i, i=1, \dots, N$ , will be very suitable<sup>5</sup> for the study of such transitions as a function of  $T$ . In our preliminary MD studies, we found that  $T^*=0.05$  was too low to trigger the changes depicted

in Fig. 1 on the time scale of our calculation.

In addition to several calculations of the type reported here, many calculations on 432 particles were also made. In this case, starting with  $V_{LJ}$  and a bcc structure, one obtains a close-packed structure with stacking faults. Repeated heating and cooling of the faulty structure finally gives a perfect fcc ordering. This implies that our dynamical equations do allow the system to monitor in configuration space the subtle local minima which correspond to stacking faults in a close-packed system.

The exploratory calculations we have reported here are an example of the way our dynamical equations make it possible to relate particle interaction to particle arrangements in ordered structures. Many other applications seem possible. Generalizing from uniform  $p_{ext}$  in Eq. (3) to a general external stress tensor, the recent work of Milstein and Farber<sup>9</sup> on the fcc-bcc transition under (100) tensile loading can be investigated as a function of temperature and of the characteristics of the pair potential. We are at present investigating this problem.

Finally, the low-temperature phase transitions in light alkali metals can also be investigated, with the dependence of the pair potential on the density of the system taken into account.<sup>3</sup>

<sup>(a)</sup>On leave of absence from the Istituto di Fisica Teorica, Miramare, Trieste, Italy.

<sup>1</sup>C. S. Hsu and A. Rahman, *J. Chem. Phys.* **71**, 4974 (1979).

<sup>2</sup>H. C. Andersen, *J. Chem. Phys.* **72**, 2384 (1980).

<sup>3</sup>D. L. Price, *Phys. Rev. A* **4**, 358 (1971); D. L. Price, K. S. Singwi, and M. P. Tosi, *Phys. Rev. B* **2**, 2983 (1970).

<sup>4</sup>J. Copley and M. Rowe, *Phys. Rev. Lett.* **32**, 49 (1974); A. Rahman, *Phys. Rev. Lett.* **32**, 52 (1974), have shown that the  $V_{Rb}$  of Ref. 3 gives a good model of rubidium.

<sup>5</sup>The structural properties generated by the Lagrangian in Eq. (1) are independent of  $W$ , as they are of  $m_i$ , the particle masses, in the classical systems under consideration. We have found in our MD studies that a higher value of  $W$  simply slows down the rate at which the effects described here occur.

<sup>6</sup>D. L. Price, *Phys. Rev. A* **4**, 358 (1971), has shown that in alkali metals the effective ion pair potentials alone give a large positive pressure which is canceled by the metallic electron contribution.

<sup>7</sup>S. Alexander and J. McTague, *Phys. Rev. Lett.* **41**, 702 (1978); J. Friedel, *J. Phys. (Paris) Lett.* **35**, L59 (1974); T. V. Ramakrishnan and M. Yussouff, *Phys. Rev. B* **19**, 2775 (1979).

<sup>8</sup>M. P. Tosi, in *Solid State Physics*, edited by H. Ehrenreich, F. Seitz, and D. Turnbull (Academic, New York, 1964), Vol. 16, p. 1.

<sup>9</sup>F. Milstein and B. Farber, *Phys. Rev. Lett.* **44**, 277 (1980).

## Effect of the Quasiparticle Mean Free Path on Poiseuille Flow in Normal Liquid $^3\text{He}$

J. P. Eisenstein,<sup>(a)</sup> G. W. Swift, and R. E. Packard

*Department of Physics, University of California, Berkeley, California 94720*

(Received 17 June 1980)

Direct observations of the effect of quasiparticle mean free path on the hydrodynamics of normal liquid  $^3\text{He}$  are presented. Both the viscosity and the mean free path are found to vary as  $T^{-2}$  down to 1.5 mK. The relevance of these observations for other  $^3\text{He}$  experiments is mentioned.

PACS numbers: 67.50.Dq, 51.20.+d

In recent years considerable interest has been focused on the properties of liquid  $^3\text{He}$  at very low temperatures.<sup>1</sup> Measurements are often interpreted using hydrodynamic theory which implicitly assumes that a continuum picture suitably describes the system. In  $^3\text{He}$ , however, the quasiparticle mean free path,  $\lambda$ , grows as  $T^{-2}$ . Below about 10 mK,  $\lambda$  can become nonnegligible compared to relevant experimental dimensions. Therefore, continuum hydrodynamics may lead to erroneous interpretation of low-temperature

$^3\text{He}$  measurements. In this paper we show how the nonzero mean free path causes departures from ordinary Poiseuille flow. Analysis of flow data allows us to determine both the viscosity and the first-order mean free path correction to the flow resistance. Without this correction one would deduce that the viscosity,  $\eta$ , does not scale as  $T^{-2}$  in apparent contrast to the Landau Fermi-liquid theory.<sup>2</sup>

In the usual treatment of Poiseuille flow through a channel one has  $\dot{V} = \Delta P / Z\eta$ , where  $\Delta P$  is the